Ultra-Relativistic Nuclear Collisions

Korinna Zapp

05. 05. 2008

Contents

1 Introduction

1.1 A QGP-Reminder

- QGP $\simeq$ state of deconfined quarks and gluons
- can be produced by heating and/or compressing hadronic matter $\rightarrow$ relativistic nuclear collisions

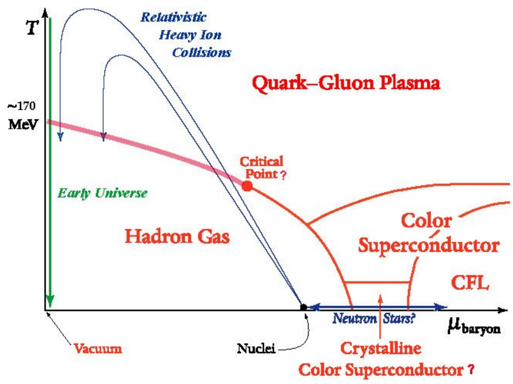

[1]

1.2 A Comment on Theoretical Tools

QCD

- correct theory of strong interaction
- but: pertubation theory only applicable at high energies/short distances (running coupling)
- in QGP at non-asymptotic temperatures coupling relativley large

Thermal field theory

- QCD in thermal systems
- but: perturbative expansion (HTL) doesn't converge very well
- application to heavy ion collisions questionable

AdS/CFT correspondence (Maldacena conjecture)

- relates strongly coupled conformal field theory to a weakly coupled type IIB string theory (supergravity)
- pro: many quantities become calculable
- con: QCD is not a conformal theory
- exciting but remains to be proven

2 Setting the Stage

2.1 Natural Units

$$\boxed{\hbar = c = k_\mathrm{B} = 1}$$

$$\Rightarrow [E] = [p] = [m] = [T] = [l^{-1}] = [t^{-1}] = \mathrm{GeV}$$

usually: $[E] = [p] = [m] = [T] = \mathrm{GeV}$
$[l] = [t] = \mathrm{fm} = 10^{-15}\,\mathrm{m}$

extremely useful: $\hbar c = 0.2\,\mathrm{GeVfm} = 1$

	J	eV	g	m^{-1}	K
J	1	$6.2 \cdot 10^{18}$	$1.1 \cdot 10^{-14}$	$3.2 \cdot 10^{25}$	$7.2 \cdot 10^{22}$
eV	$1.6 \cdot 10^{-19}$	1	$1.8 \cdot 10^{-33}$	$5.1 \cdot 10^{6}$	$1.2 \cdot 10^{4}$
g	$9.0 \cdot 10^{13}$	$5.6 \cdot 10^{32}$	1	$2.8 \cdot 10^{39}$	$6.5 \cdot 10^{36}$
m^{-1}	$3.2 \cdot 10^{-26}$	$2.0 \cdot 10^{-7}$	$3.5 \cdot 10^{-40}$	1	$2.2 \cdot 10^{-3}$
K	$1.4 \cdot 10^{-23}$	$8.6 \cdot 10^{-5}$	$1.5 \cdot 10^{-37}$	$4.4 \cdot 10^{2}$	1

2.2 Coordinates and Useful Quantities

Coordinates and Useful Quantities

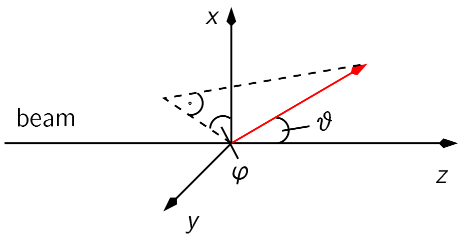

1-Particle Observables

longitudinal momentum: $p_{||} = |\vec{p}| \cos\vartheta$
transverse momentum: $p_\perp = |\vec{p}| \sin\vartheta$
transverse mass: $m_\perp = \sqrt{p_\perp^2 + m^2}$
rapidity: $y = \tanh^{-1}(\beta_{||}) = \frac{1}{2} \ln\left(\frac{E+p_{||}}{E-p_{||}}\right)$
pseudo-rapidity: $\eta = -\ln\left(\tan\frac{\vartheta}{2}\right) = \frac{1}{2} \ln\left(\frac{p+p_{||}}{p-p_{||}}\right)$

for $E \gg m$: $y \simeq \eta$

Global Observables

transverse energy: $E_\perp = \sum_i E_i \sin\vartheta_i$

excitation energy: $E^* = E_{\rm cm} - N_{\rm part} m_{\rm N} = (\gamma_{\rm beam} N_{\rm part,beam} + \gamma_{\rm target} N_{\rm part,target}) m_{\rm N} - N_{\rm part} m_{\rm N}$ kinetic energy of participating nucleons $\rightarrow$ energy of the produced matter

isotropic source: $E_\perp = \frac{\pi}{4} E^*$

zero-degree energy: $E_{\rm ZD}$: energy deposited in small solid angle around beam axis $\rightarrow$ sensitive to number of projectile spectator nucleons ideally: $\frac{E_{\rm ZD}}{E_{\rm beam}} = \frac{N_{\rm spec}}{A}$

$\Rightarrow$ $E_\perp$ and $E_{\rm ZD}$ (E^*) complementary

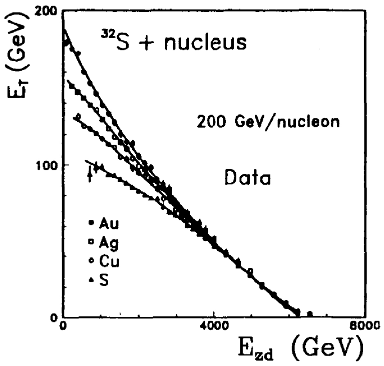

[2]

Rapidity

rapidity: relativistic analogue of (longitudinal) velocity

$$\begin{aligned}
\beta &= \frac{\beta_1 + \beta_2}{1 + \beta_1 \beta_2} \\
y &= \tanh^{-1} \beta \\
&= \tanh^{-1} \left(\frac{\beta_1 + \beta_2}{1 + \beta_1 \beta_2} \right) \\
&= \tanh^{-1} \beta_1 + \tanh^{-1} \beta_2 \\
&= y_1 + y_2
\end{aligned}$$

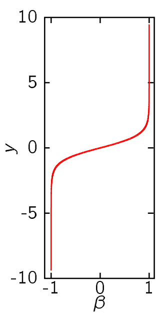

$\Rightarrow$ *The shape of rapidity distributions is invariant under Lorentz-transformations.*

Accelerators and Beam Rapidity

AGS: $E_{\rm beam} = 11\,$A GeV Au+Au fixed target

SPS: $E_{\rm beam} = 158\,$A GeV Pb+Pb fixed target

RHIC: $\sqrt{s_{\rm NN}} = 200\,$GeV Au+Au collider

LHC: $\sqrt{s_{NN}} = 5.5\,\text{TeV}$ Pb+Pb collider

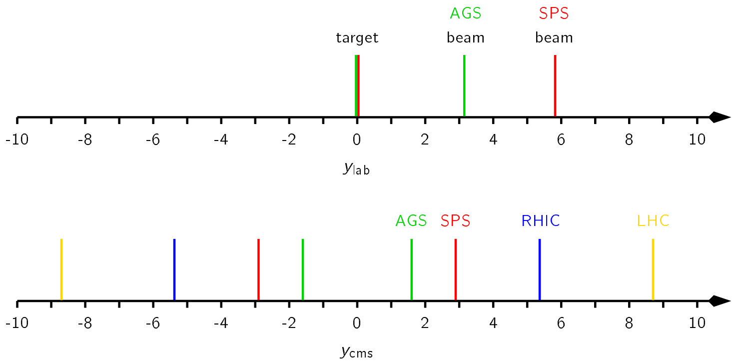

2.3 Stages of a Nuclear Collision

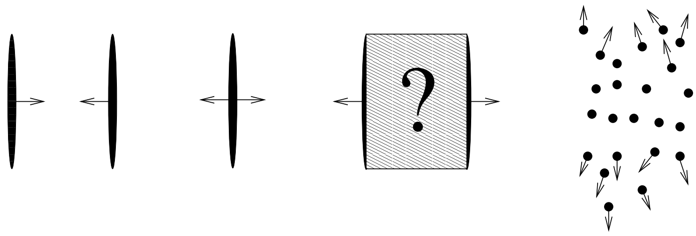

(a) (b) (c) (d)

(a) Lorentz-contracted nuclei

(b) nuclei overlap, scatterings occur

(c) nucleus remnants recede from interaction region leaving a dense and hot system behind

(d) system expands, cools and hadronises, hadrons scatter and resonances decay

2.4 Geometry

Centrality

b: impact parameter

$$\text{centrality} = \frac{\sigma}{\sigma_{\text{geo}}} \simeq \frac{\int_0^b b' \mathrm{d}b'}{\int_0^{2R_A} b' \mathrm{d}b'} \propto b^2$$

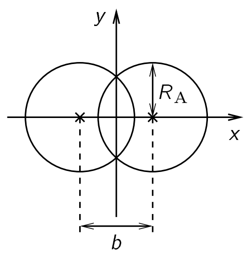

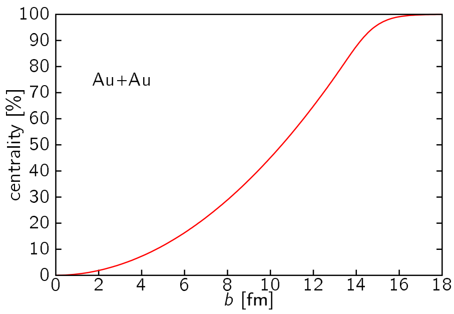

[3]

Glauber-models

- characterise collision by
  - number of participating nucleons ($N_{\text{part}}(b)$)
  - number of binary nucleon-nucleon collisions ($N_{\text{bin}}(b)$)
- rule of thumb:
  - soft (low momenta) particle production scales with N_{part}
  - hard (high momentum transfer) processes scale with N_{bin}

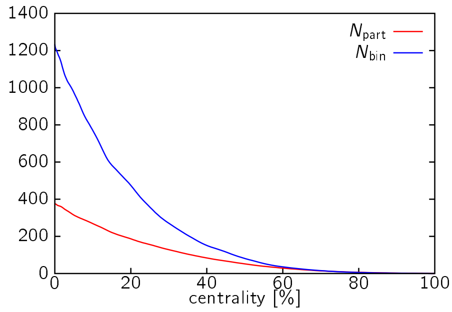

[3]

3 An Example of an Experiment

3.1 Challenges

General Complications

- QGP not directly observable
- have to infer QGP properties from hadronic final state
- complicated space-time evolution
- comlpex multi-particle dynamics

Experimental Challenges

- high multiplicity (RHIC: up to ~ 4000 charged particles)
- many measurements have huge background
- this background contains structures and correlations
- it fluctuates

3.2 An Example for an Experiment: STAR

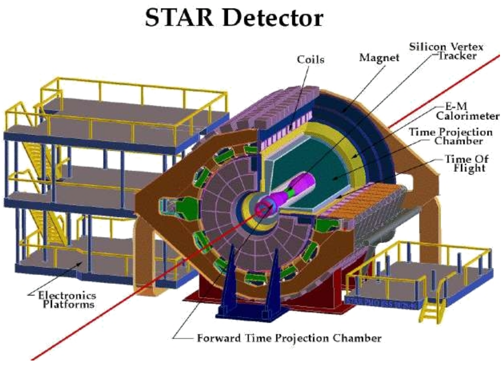

[4]

Silicon Vertex Tracker: position and momentum

Time Projection Chamber: momentum and position

Time Of Flight: velocity

E-M Calorimeter: energy

$\Rightarrow$ combining information from different subdetetors allows for particle identification

4 Aspects of Relativistic Nuclear Collisions

4.1 Centrality

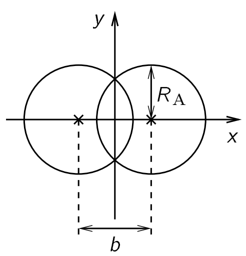

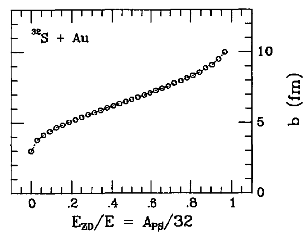

[2]

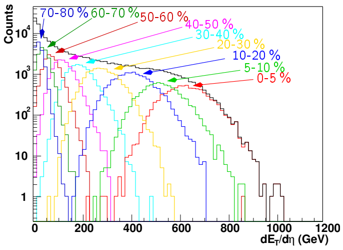

[5]

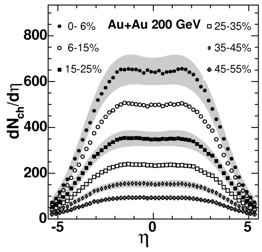

[6]

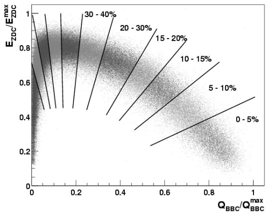

[7]

- Q_{BBC}: charge in Beam Beam Counter (detector at $3 < |\eta| < 4$ measuring number of charged particles)

- complication: imcomplete measurement of spectators

Collisions with increasing centrality have

- increasing activity away from beam rapidity (transverse energy, number of produced particles, total charge etc.).
- decreasing activity near beam rapidity, i.e. decreasing number of spectator nucleons.

⇒ use a combination of the two to experimentally determine centrality

4.2 Particle Production

Stopping

nuclear stopping power: amount of kinetic energy lost by projectiles

⇒ stopping means that protons get shifted to midrapidity

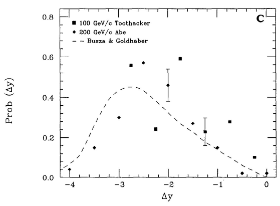

[8]

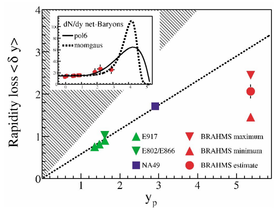

[9]

⇒ mean rapidity shift of projectiles: $\Delta y \simeq 2$

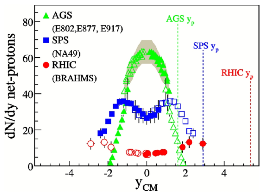

[10]

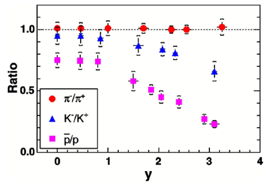

[10]

$\Rightarrow$ inceasing beam energy we go from stopping to transparency

- valence quark part of wave function gets more and more Lorentz-contracted while sea cannot become smaller than $\sim 1\,\mathrm{fm}$ (uncertainty principle) $\rightarrow$ collisions at high energy dominated by sea-sea interactions

Total Energy

$$E = m_\perp \cosh y \Rightarrow E_{\mathrm{tot}} = \sum_{\mathrm{species}} \int \mathrm{d}y \frac{\mathrm{d}N}{\mathrm{d}y} \langle m_\perp \rangle \cosh y$$

particle	energy [GeV]
p	3108
$\bar{p}$	428
K^+	1628
K^-	1093
π^+	5888
π^-	6117
π^0	6004
n	3729
$\bar{n}$	513
K^0	1628
$\bar{K}^0$	1093
Λ	1879
$\bar{\Lambda}$	342

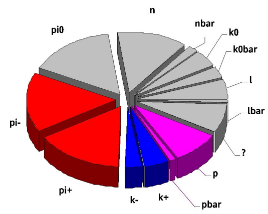

[12]

total: 33.4 TeV
$E_{\mathrm{beam}} \cdot N_{\mathrm{part}} = 35\,\mathrm{TeV}$
produced: 24.8 TeV
$\Rightarrow$ 74 % of beam energy goes into particle production

Rapidity Distribution

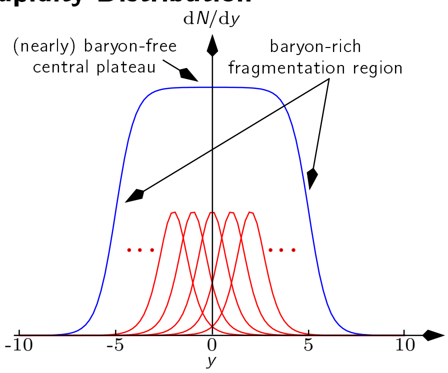

- isotropic particle source at rest: $\frac{\mathrm{d}N_1}{\mathrm{d}\cos\vartheta} = \frac{N_{1,\mathrm{tot}}}{2}$

- $y = \frac{1}{2} \ln \left(\frac{E + p\cos\vartheta}{E - p\cos\vartheta} \right)$

  $\Rightarrow \cos\vartheta = \frac{E}{p} \tanh y$

  $\Rightarrow \frac{\mathrm{d}N_1}{\mathrm{d}y} = \frac{\mathrm{d}N_1}{\mathrm{d}\cos\vartheta} \frac{\mathrm{d}\cos\vartheta}{\mathrm{d}y}$

  $= \frac{N_{1,\mathrm{tot}}}{2} \frac{E}{p} \mathrm{sech}^2 y$

- moving isotropic source: $\frac{\mathrm{d}N_1}{\mathrm{d}y} = \frac{N_{1,\mathrm{tot}}}{2}\frac{E}{p}\mathrm{sech}^2(y + y_\mathrm{s})$
- picture of nuclear collision: particles need proper time τ_de to form $\rightarrow$ time-dilated in lab frame $\gamma\tau_\mathrm{de}$ $\rightarrow$ superposition if independent moving sources
- $\frac{\mathrm{d}N}{\mathrm{d}y} = \int\limits_{-y_\mathrm{max}}^{y_\mathrm{max}} \mathrm{d}y' \frac{\mathrm{d}N_1}{\mathrm{d}y}(y + y') \propto \tanh(y + y_\mathrm{max}) - \tanh(y - y_\mathrm{max})$

Space-Time Picture

- particle formation time: $t = \gamma\tau_\mathrm{de}$ from moment of projectile overlap at $t = 0$ and $z = 0$
- particles at rest ($\gamma = 1$) are formed at midrapidity and at $z = 0$
- moving particles are formed at higher rapidity and travel a distance $\beta/\gamma\tau_\mathrm{de}$ before formation

$\Rightarrow$ Particles with high rapidity are produced at high z

$\Rightarrow$ *The rapidity is related to the point of particle emission (in coordinate space).*

$$y = \frac{1}{2}\ln\left(\frac{E + p_{||}}{E - p_{||}}\right) = \frac{1}{2}\ln\left(\frac{\gamma m + \gamma m v}{\gamma m - \gamma m v}\right) = \frac{1}{2}\ln\left(\frac{t + z}{t - z}\right) = Y$$

Y: space-time rapidity

NB: We habe ignored the transverse expansion.

4.3 Density

$$\text{Bjorken's density estimate:} \quad \epsilon_0 = \frac{1}{\pi R^2 \tau_0} \left.\frac{\mathrm{d}E_\perp}{\mathrm{d}\eta}\right|_{\eta\simeq 0}$$

$\tau = \sqrt{t^2 - z^2}$: proper time
τ_0 : equilibration time ($\tau_0 \simeq 0.2 \ldots 1\,\mathrm{fm}$)
$\epsilon_0 = \epsilon(\tau_0)$: early energy density

$$\left.\frac{\mathrm{d}E_\perp}{\mathrm{d}\eta}\right|_{\eta=0} \simeq \left.\frac{\mathrm{d}E_\perp}{\mathrm{d}y}\right|_{y=0} = \pi R^2 \epsilon(\tau) \left.\frac{\mathrm{d}z}{\mathrm{d}y}\right|_{y=0} = \pi R^2 \epsilon(\tau)\tau$$

$$\epsilon\tau = \epsilon_0\tau_0 \text{ from entropy conservation}$$

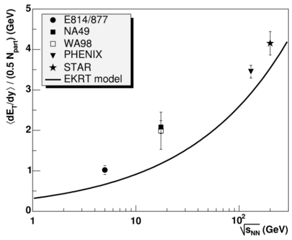

[5]

- for $\tau_0 = 1\,\mathrm{fm}$
  - AGS: $\epsilon_0 = 1.4\,\mathrm{GeV\,fm^{-3}}$
  - SPS: $\epsilon_0 = 3\,\mathrm{GeV\,fm^{-3}}$
  - RHIC: $\epsilon_0 = 5\,\mathrm{GeV\,fm^{-3}}$
- esimated density needed to form QGP $1\,\mathrm{GeV\,fm^{-3}}$

4.4 Transverse Expansion Velocity

$$\text{thermal source:} \quad \frac{\mathrm{d}N}{m_\perp \mathrm{d}m_\perp} \propto \exp\left(\frac{m_\perp - m_0}{T_{\mathrm{kin}}}\right)$$

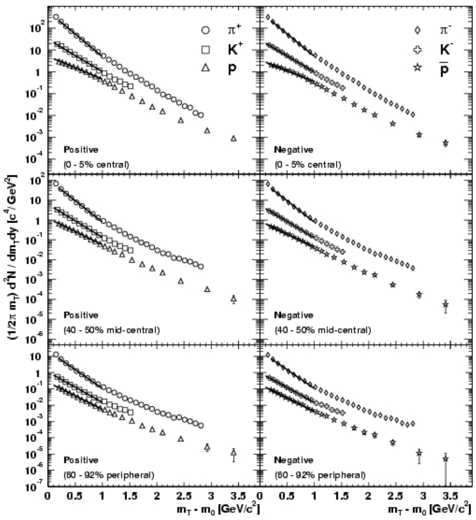

[7]

- T_{kin}: kinetic freeze-out temperature ('temperature at last interaction')
- spectrum ot exactly exponential
- inverse slope T_{kin} depends on particle mass

⇒ characteristic of transverse flow: $T_{kin}^{\mathrm{eff}} \simeq T_{kin} + m_0 \beta_r^2/2$

⇒ need a hydrodynamic calculation

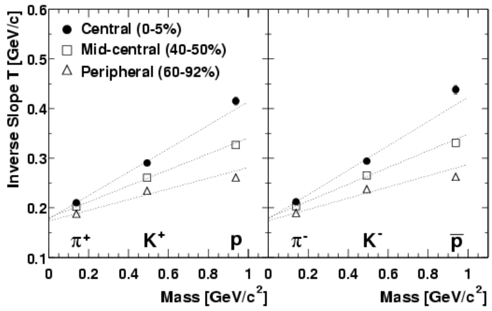

[7]

$$\frac{\mathrm{d}N}{m_\perp \mathrm{d}m_\perp} \propto \int_0^R r \mathrm{d}r \, m_\perp I_0 \left(\frac{p_\perp \sinh \rho}{T_{kin}} \right) K_1 \left(\frac{p_\perp \cosh \rho}{T_{kin}} \right)$$

$$\text{with} \quad \rho = \tanh^{-1} \beta_\mathrm{r} \quad \text{and} \quad \beta_\mathrm{r}(r) = \beta_\mathrm{s} \left(\frac{r}{R} \right)^n \;\; ; \; 0 \le r \le R$$

$n \approx 1$ — analogous to Hubble expansion

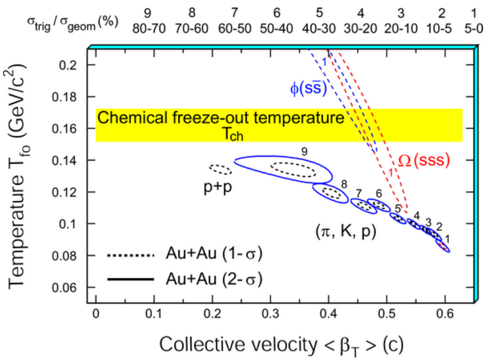

[11]

4.5 Equation of State

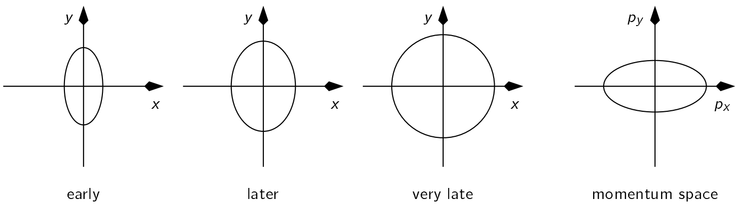

- mean free path $\ll$ system size $\to$ hydrodynamical description
- pressure gradient steeper in x-direction
- collective flow develops preferentially in x-direction
- particle distribution shows azimuthal anisotropy

- anisotopy directly sensitive to equation of state
- mostly sensitive to early times, when eccentricity is largest

$$E\frac{d^3N}{d^3p} = \frac{d^2N}{2\pi p_\perp dp_\perp dy}\left(1+\sum_{n=1}^{\infty}2v_n\cos(n\phi)\right)$$

elliptic flow: $v_2 = \langle\cos(2\phi)\rangle$

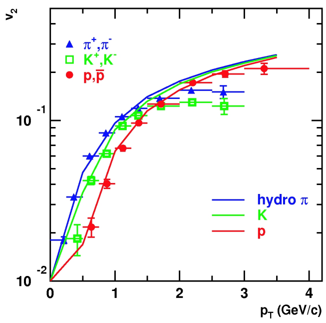

[13]

- hydrodynamic calculations with QGP EOS do good job at top SPS energies and RHIC
- suggests thermalisation and QGP formation

4.6 Spatial Extension

- Hanbury Brown - Twiss interferometry: interferometry of identical particles (originally used to determine size of stars)
- measure momenta $\vec{k}_1$ and $\vec{k}_2$ of two pions emitted from $\vec{x}_1$ and $\vec{x}_2$, respectively, at different positions
- indistinguishable particles $\rightarrow$ interference
- transition probability:

$$\begin{aligned}|\Psi_{12}|^2 &= \frac{1}{2V^2}\left|e^{-i\vec{k}_1\cdot\vec{x}_1}e^{-i\vec{k}_2\cdot\vec{x}_2}+e^{-i\vec{k}_1\cdot\vec{x}_2}e^{-i\vec{k}_2\cdot\vec{x}_1}\right|^2\\ &= \frac{1}{V^2}\left(1+\cos(\Delta\vec{k}\cdot\Delta\vec{x})\right)\end{aligned}$$

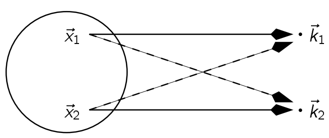

- probability of observing $\vec{k}_1$ and $\vec{k}_2$ in emission from continuous source

$$P(\vec{k}_1,\vec{k}_2) = \frac{1}{2}\int d^3x_1 d^3x_2 \rho(\vec{x}_1)\rho(\vec{x}_2)|\Psi_{12}|^2$$

- probability of observing a single particle with $\vec{k}_i$

$$P(\vec{k}_i) = \int \mathrm{d}^3 x_i \rho(\vec{x}_i) \| \langle \vec{k}_i | \vec{x}_i \rangle |^2$$

- correlation function

$$\begin{aligned} C_2 &\equiv \frac{\mathrm{d}^6 N}{\mathrm{d}^3 k_1 \mathrm{d}^3 k_2} \left(\frac{\mathrm{d}^3 N}{\mathrm{d}^3 k_1} \frac{\mathrm{d}^3 N}{\mathrm{d}^3 k_2} \right)^{-1} = \frac{2P(\vec{k}_1, \vec{k}_2)}{P(\vec{k}_1) P(\vec{k}_2)} \\ &= 1 + |\tilde{\rho}(\Delta \vec{k})|^2 \end{aligned}$$

  where $\tilde{\rho}$ is the Fourier transform of the density distribution

$\Rightarrow$ can infer size of source from correlation function

- in practice: fit a 3d Gaussian to data
- life is more complicated and more interesting with an expanding source
  - radii depend on transverse momentum of pair
  - $R_{\mathrm{out}}/R_{\mathrm{side}} > 1$ for long duration of hadron emission

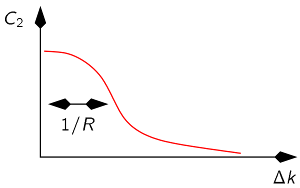

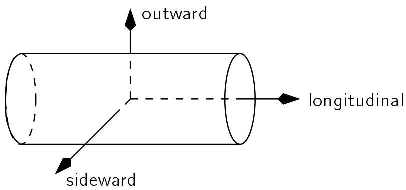

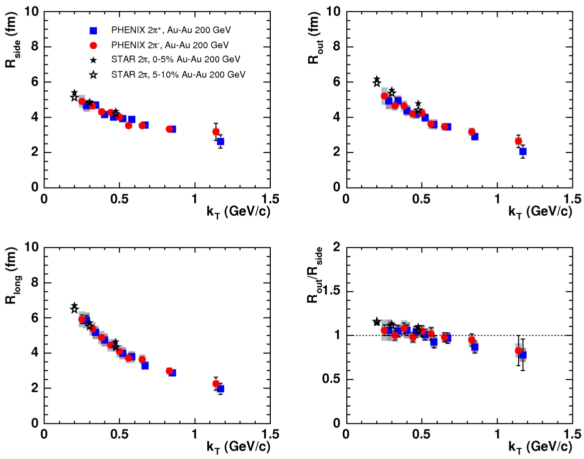

[13]

- transverse rms radii larger than nuclei
- radii decrease with pair transverse momentum

$\Rightarrow$ extended, expanding source (β_r consistent with $m_\perp$ spectra)

- $R_{\mathrm{out}}/R_{\mathrm{side}} \sim 1$

5 Summary

What we have learned about the properties of the hot and dense matter produced in relativistic nuclear collisions:

- low beam energies: stopping; high beam energies: transparency (proton & antiproton rapidity distributions)
- longitudinal expasion (rapidity distribution of charged particles)
- transverse expansion ($m_\perp$-spectra, HBT radii, elliptic flow)
- at top SPS energies and RHIC: QGP formation (density, elliptic flow)
- early thermalisation (elliptic flow)

References

[1] from a sketch by K. Rajagopal

[2] J. Stachel and G. R. Young "Relativistic heavy ion physics at CERN and BNL," Ann. Rev. Nucl. Part. Sci. **42** (1992) 537.

[3] `http://www-linux.gsi.de/~misko/overlap/interface.html`

[4] `http://www.star.bnl.gov/central/experiment`

[5] J. Adams *et al.* [STAR Collaboration] "Measurements of transverse energy distributions in Au + Au collisions at s(NN)**(1/2) = 200-GeV," Phys. Rev. C **70** (2004) 054907 [arXiv:nucl-ex/0407003].

[6] B. B. Back *et al.* "The PHOBOS perspective on discoveries at RHIC," Nucl. Phys. A **757** (2005) 28 [arXiv:nucl-ex/0410022].

[7] S. S. Adler *et al.* [PHENIX Collaboration] "Identified charged particle spectra and yields in Au + Au collisions at s(NN)**(1/2) = 200-GeV," Phys. Rev. C **69** (2004) 034909 [arXiv:nucl-ex/0307022].

[8] W. Busza and R. Ledoux, "ENERGY DEPOSITION IN HIGH-ENERGY PROTON NUCLEUS COLLISIONS," Ann. Rev. Nucl. Part. Sci. **38** (1988) 119.

[9] I. G. Bearden *et al.* [BRAHMS Collaboration], "Nuclear stopping in Au + Au collisions at s(NN)**(1/2) = 200-GeV," Phys. Rev. Lett. **93** (2004) 102301 [arXiv:nucl-ex/0312023].

[10] I. Arsene *et al.* [BRAHMS Collaboration] "Quark gluon plasma and color glass condensate at RHIC? The perspective from the BRAHMS experiment," Nucl. Phys. A **757** (2005) 1 [arXiv:nucl-ex/0410020].

[11] J. Adams *et al.* [STAR Collaboration] "Experimental and theoretical challenges in the search for the quark gluon plasma: The STAR collaboration's critical assessment of the evidence from RHIC collisions," Nucl. Phys. A **757** (2005) 102 [arXiv:nucl-ex/0501009].

[12] R. Debbe [BRAHMS Collaboration], "BRAHMS Overview," J. Phys. Conf. Ser. **50** (2006) 42 [arXiv:nucl-ex/0504015].

[13] K. Adcox *et al.* [PHENIX Collaboration] “Formation of dense partonic matter in relativistic nucleus nucleus collisions at RHIC: Experimental evaluation by the PHENIX collaboration,” Nucl. Phys. A **757** (2005) 184 [arXiv:nucl-ex/0410003].